Article

Discovery Medicine 2025; 37(195): 737–749
https://doi.org/10.24976/Discov.Med.202537195.64

A Potential Link Between Early Onset Reactive Astrogliosis and Adult-Onset Dysfunction of Leptin Signaling in Polyubiquitin Gene *Ubb* Knockout Mice

Jin-Sil Bae[1,†], Sekee Yoon[1,†], Taek-Yeong Kim[1], Kwon-Yul Ryu[1,*]

[1]Department of Life Science, University of Seoul, 02504 Seoul, Republic of Korea
*Correspondence: kyryu@uos.ac.kr (Kwon-Yul Ryu)
[†]These authors contributed equally.
Published: 20 April 2025

Background: Polyubiquitin gene *Ubb* knockout (KO) mice exhibit early onset reactive astrogliosis and adult-onset hypothalamic neurodegeneration with obesity. However, it remains unknown why the obesity phenotype only manifests in adulthood and why mice are smaller at an early age. Therefore, this study aimed to identify the link between neuroinflammation at an early age and adult-onset leptin signaling dysfunction in *Ubb* KO mice.

Methods: To investigate neuroinflammatory marker expression in the hypothalamus of *Ubb* KO mice, RNA-seq analysis and quantitative reverse transcription-polymerase chain reaction were used. Moreover, astrocytes isolated from postnatal brains were cultured and pure astrocytes were obtained by magnetic-activated cell sorting. Furthermore, mice were challenged with lipopolysaccharide (LPS) to induce upregulation of neuroinflammatory markers, including lipocalin-2 (LCN2). Leptin signaling was examined through the administration of leptin via intraperitoneal or intracerebroventricular injection, followed by monitoring of relevant proteins using immunofluorescence and western blot analyses.

Results: In *Ubb* KO mice, reactive astrogliosis occurred at an early age and increased the expression of *Lcn2* and other neuroinflammatory markers. Upon exposure to LPS, these levels showed upward trends; however, they were comparable with those in wild-type mice, suggesting that *Ubb* KO mice were under intrinsic inflammatory stress. In adulthood, leptin signaling dysfunction was observed owing to elevated levels of negative regulators, such as suppressor of cytokine signaling-3 (SOCS3) and forkhead box protein O1 (FOXO1), possibly as a result of chronic neuroinflammation.

Conclusion: This study demonstrates that *Lcn2* expression is increased in young *Ubb* KO mice. Although leptin signaling is intact at an early age, high LCN2 levels may contribute to reduced daily food intake and lower body weight. Chronic neuroinflammation resulting from reactive astrogliosis persists into adulthood, leading to leptin signaling dysfunction. This is most likely a result of elevated levels of SOCS3 and FOXO1, both of which are negative regulators of leptin signaling.

Keywords: ubiquitin; polyubiquitin gene *Ubb*; lipocalin-2; reactive astrogliosis; neuroinflammation; leptin signaling

Introduction

Ubiquitin (Ub) plays a crucial role in protein homeostasis and various cellular processes, including the degradation of misfolded proteins via the proteasome [1–3]. Target proteins are ubiquitinated via a cascade involving three classes of enzymes: Ub-activating enzymes (E1), Ub-conjugating enzymes (E2), and Ub ligases (E3) [4]. Moreover, Ub can be removed from target proteins by deubiquitinating enzymes [5]. In eukaryotes, Ub proteins are encoded by two types of Ub genes, Ub-ribosomal fusion genes and polyubiquitin genes [6–8].

Polyubiquitin gene *Ubb* knockout (KO) mice exhibit two prominent phenotypes: early onset reactive astrogliosis at one month of age, and adult-onset hypothalamic neurodegeneration accompanied by increased fat content and elevated serum leptin levels at 3–4 months of age [9]. In adulthood, *Ubb* KO mice appear obese; hence, this state is defined as an adult-onset obesity phenotype [9]. Interestingly, metabolic abnormalities, including reduced energy expenditure and activity, are observed as early as one month of age and persist into adulthood [10]. Furthermore, *Ubb* KO mice are born small with reduced body weight in the early stages of life; however, their body weight eventually reaches that of control mice (wild-type [WT] and heterozygous mutants) by adulthood [9].

Furthermore, regardless of age, the body weight-normalized food intake of *Ubb* KO mice is identical to that of WT mice under *ad libitum* feeding conditions [9]. Body weight and food intake data suggest that *Ubb* KO mice consume less food or are hypophagic when they are young but gradually increase their daily food intake, ultimately consuming a similar amount of food as WT mice when they reach adulthood. Thus, the adult-onset obesity phenotype

was not a result of increased body weight or hyperphagic behavior. However, the reason the mice are hypophagic and smaller at an early age, and the mechanism by which they become obese in adulthood remains unknown.

Energy homeostasis, including food intake, energy expenditure, and body weight, is regulated by hypothalamic neural circuits primarily through neurons that express leptin receptors [11,12]. To investigate whether leptin signaling was intact or impaired in *Ubb* KO mice, the phosphorylation of signal transducer and activator of transcription-3 (STAT3) in the hypothalamus was examined in this study. The binding of leptin to its receptor activates Janus kinase 2, which phosphorylates the receptor, leading to recruitment and phosphorylation of STAT3 [13]. The phosphorylated STAT3 (pSTAT3) dimers translocate to the nucleus and promote the expression of anorexigenic neuropeptides, such as pro-opiomelanocortin, to suppress appetite [13].

Activated astrocytes increase the expression of pan, A1, and A2 markers [14]. Pan markers increase with astrocyte activation, whereas A1 markers generally increase when astrocytes are neurotoxic and A2 markers increase when they are neuroprotective [15]. Lipopolysaccharide (LPS) treatment increases pan and A1 but not A2 markers [14]. Even under the same conditions of inflammatory stress, each activated astrocyte may have a unique transcriptomic profile [16]. Thus, the dichotomous A1/A2 classification is no longer accepted; however, activated astrocytes can exist in two distinct states that may coexist [17,18]. Lipocalin-2 (LCN2), which is secreted by reactive astrocytes and is a pan-marker, exerts anorexigenic effects, suppresses appetite, and reduces daily food intake [19–21]. In addition, chronic neuroinflammation has been implicated in the upregulation of the suppressor of cytokine signaling-3 (SOCS3), a protein with anti-inflammatory properties that also serves as a negative regulator of leptin signaling [13,22–27]. Thus, the reasons for impaired leptin signaling in adult *Ubb* KO mice were investigated in this study. In addition, forkhead box protein O1 (FOXO1), a transcription factor that competes with pSTAT3, inhibits the expression of anorexigenic neuropeptides and serves as a negative regulator of leptin signaling [28].

In this study, *Lcn2* expression was elevated in one-month-old *Ubb* KO mice, suggesting that young *Ubb* KO mice exhibit anorexigenic behavior, which may explain their smaller size. By 3–4 months of age, *Lcn2* expression in *Ubb* KO mice was no longer elevated and was comparable with that in WT mice, suggesting that adult *Ubb* KO mice may no longer be anorexigenic. Moreover, reactive astrogliosis observed at one month of age likely contributes to chronic neuroinflammation, which increases *Socs3* expression in adulthood. Although leptin signaling remains intact during the early stages, it is impaired in adulthood. This is most likely a result of elevated SOCS3 levels. This dysfunction may explain the increased serum leptin levels and obesity observed in adult *Ubb* KO mice.

Therefore, this study suggests a potential link between early onset reactive astrogliosis and adult-onset dysfunction of leptin signaling, which contributes to the obesity phenotype observed in adult *Ubb* KO mice.

Materials and Methods

Mouse Studies

Ubb heterozygous mutant mice were originally generated at the Ron Kopito Laboratory of Stanford University. *Ubb* heterozygous mutant mice (five-month-old, 10 males [body weight ~35 g] and four females [body weight ~25 g]) were transferred to the animal facility at the University of Seoul, where they were maintained. WT and *Ubb* KO mice were generated by breeding *Ubb* heterozygous mutant mice. The mice were housed in individually ventilated cages with free access to food and water, at a temperature range of 24–26 °C and a humidity range of 40–60%. During fasting, food and bedding were withheld, but water was provided.

If necessary, the mice were anesthetized with 1.25% or 2.5% avertin (20 µL/g body weight) via intraperitoneal (IP) injection. A concentration of 1.25% avertin was used for young (one-month-old) mice, whereas 2.5% avertin was used for adult (three- to four-month-old) mice. A 100% avertin stock solution was prepared by mixing 5 mL of 2-methyl-2-butanol (240486; Sigma-Aldrich, St. Louis, MO, USA) and 5 g 2,2,2-tribromoethanol (48402; Sigma-Aldrich, St. Louis, MO, USA) overnight at room temperature (RT). Next, the stock solution was then diluted to 1.25% or 2.5% avertin with phosphate-buffered saline (PBS) overnight at RT until no crystals were present, after which it was filtered through a 0.22 µm membrane and stored at 4 °C.

The mice were divided into four groups: group 1, young (one-month-old) WT mice with body weight ~15 g; group 2, young (one-month-old) *Ubb* KO mice with body weight ~12 g; group 3, adult (three- to four-month-old) WT mice with body weight ~30 g; and group 4, adult (three- to four-month-old) *Ubb* KO mice with body weight ~28 g. In each group, mice were randomly selected, regardless of sex. When necessary, these groups were further subdivided into vehicle-treated (PBS) and drug-treated (LPS or leptin) subgroups. For euthanasia, mice were placed in a chamber and exposed to a gradual flow of CO_2 until euthanasia was achieved.

Mouse Injection

For intracerebroventricular (ICV) injection of leptin (498-OB-01M; R&D Systems, Minneapolis, MN, USA), a Hamilton syringe (701RN; Hamilton Company Inc, Reno, NV, USA) was positioned 0.5 mm posterior and 0.1 mm lateral to the bregma, and 3.0 mm ventral to the surface of the skull using a stereotaxic instrument (JD-SI-02P; Jeungdo Bio & Plant, Seoul, Korea). One µL of leptin (1 µg/µL) was

injected over a 5 min period. After the injection, the skin was sutured with a surgical thread. Mice were kept at 40 °C until they regained consciousness. For IP injection of LPS (L2630-10MG; Sigma-Aldrich, St. Louis, MO, USA), the mice were administered 5 mg of LPS per kg of body weight dissolved in PBS. For systemic exposure, LPS (0.5 mg/mL) was injected 24 h before the experiment.

RNA-Seq Analysis

RNA-seq analysis was carried out by LAS Inc (https://www.las.kr). Briefly, total RNA was isolated from the hypothalamus of mice using TRI reagent (TR118; Molecular Research Center, Cincinnati, OH, USA), and an mRNA sequencing library was prepared using the MGIEasy RNA directional library prep kit (1000006385; MGI Tech, Shenzhen, China) according to the manufacturer's protocol. After mRNA purification, it was fragmented, complementary DNA (cDNA) was prepared using reverse transcriptase, and the final cDNA library was generated. The library was processed to create DNA nanoballs (DNBs), and the prepared DNBs were sequenced using an MGIseq system (MGI-G400, MGI Tech, Shenzhen, China) with 100 bp paired-end reads. Expression quantification, differentially expressed gene (DEG) analysis, and visualization of results were performed by LAS Inc (https://www.las.kr).

Floating Sections of the Brain and Immunofluorescence Analysis

To investigate STAT3 phosphorylation, mice were fasted for 24 h, and recombinant leptin (0.1 mg/mL, 1 mg/kg body weight; 498-OB-01M; R&D Systems, Minneapolis, MN, USA) was injected intraperitoneally. After 1 h, mice were perfused with 4% paraformaldehyde/PBS, and the brains were dissected, post-fixed for 18 h, and equilibrated with 30% sucrose/PBS for 48 h. The brains were embedded in OCT media (3801480; Leica Biosystems, Wetzlar, Germany) at –20 °C. Coronal brain sections (25 µm thick) were prepared using a cryostat (Leica CM1800, Leica Biosystems, Wetzlar, Germany). Sections containing the hypothalamic area (1.2–3.3 mm posterior to bregma) were collected, floated on cryo-preservative media (25% glycerol and 30% ethylene glycol in PBS), and stored at –20 °C until use.

The floating sections were washed with Tris-buffered saline (TBS), transferred onto (3-aminopropyl) triethoxysilane (APTES; 440140-100ML; Sigma-Aldrich, St. Louis, MO, USA)-coated glass slides, and outlined using a PAP pen. For immunofluorescence analysis of pSTAT3, floating sections were pretreated with 1% NaOH/TBS for 15 min and permeabilized with 0.3% Triton X-100/TBS for 15 min. After blocking for 1 h in 3% bovine serum albumin (BSA)/0.3% Triton X-100/TBS at RT, the sections were incubated with a pSTAT3 (Y705) antibody (1:100; 9131; Cell Signaling Technology, Danvers, MA, USA) in a blocking solution containing PhosStop (4906845001; Roche, Basel, Switzerland) for 16 h. After washing with 0.3% Triton X-100/TBS, the sections were subsequently incubated with Alexa Flour™ 555 goat anti-rabbit immunoglobulin G (IgG) (A21428; 1:200; Thermo Fisher Scientific, Waltham, MA, USA) with 0.1 µg/mL of bisbenzimide (Hoechst 33342; B2261-25MG; Sigma-Aldrich, St. Louis, MO, USA) for 1 h at RT. After washing, the sections were dried and mounted on slides using the Permount solution (SP15-100; Fisher Chemicals, Zurich, Switzerland). Immunofluorescent images were obtained using an LSM 800 Airyscan confocal microscope with ZEN Blue software (version 2.6; Carl Zeiss, Oberkochen, Germany).

Quantitative Reverse Transcription-Polymerase Chain Reaction (qRT-PCR) Analysis

Total RNA was isolated from the hypothalamus using TRI reagent (TR118; Molecular Research Center, Cincinnati, OH, USA) and treated with DNase I (18068015; Thermo Fisher Scientific, Waltham, MA, USA) to remove genomic DNA contamination. For cDNA synthesis, 2 µg of total RNA was reverse-transcribed using SuperiorScript II reverse transcriptase (RT005M, Enzynomics, Daejeon, Korea). The qRT-PCR was performed using 5 µL of cDNA, a SYBR Master Mix (RT500M; Enzynomics, Daejeon, Korea), and the iCycler system with iCycler iQ software (version 2.0, Bio-Rad, Hercules, CA, USA). We converted cycle threshold (Ct) values to mRNA expression levels of the gene of interest (GOI; $2^{-Ct,\ GOI}$). The mRNA expression levels were normalized by dividing them by the expression level of glyceraldehyde-3-phosphate dehydrogenase (*Gapdh*; $2^{-Ct,\ GOI}/2^{-Ct,\ Gapdh}$). The primers used for qRT-PCR and their sequences are listed in Table 1.

Tissue Lysis and Western Blot Analysis

Hemi-hypothalamic tissues were homogenized with 100 µL of lysis buffer (50 mM Tris-Cl pH 7.4, 150 mM NaCl, 5 mM ethylenediaminetetraacetic acid [EDTA], 1% Triton X-100, 0.5% deoxycholic acid), containing protease inhibitors (1 µg/mL aprotinin, 1 µg/mL leupeptin, and 1 mg/mL phenylmethylsulfonyl fluoride) and a phosphatase inhibitor cocktail (QTPPI1041; Quartett, Berlin, Germany) at 4 °C. Tissue lysates were centrifuged at 13,000 rpm for 10 min, the supernatant was collected, and the protein concentration was measured using a Pierce™ BCA protein assay kit (23225; Thermo Fisher Scientific, Waltham, MA, USA). Samples were boiled in sodium dodecyl-sulfate (SDS) loading buffer, and 15–50 µg of tissue lysates were used for SDS-polyacrylamide gel electrophoresis. Proteins were transferred to polyvinylidene difluoride membranes and blocked with 3% BSA in TBS containing 0.05% Tween 20 (TBST) for 1 h at RT.

Western blot analysis was performed using anti-LCN2 (1:1000; PA5-79590; Invitrogen, Carlsbad, CA, USA), anti-SOCS3 (1:50; C204; IBL America, Minneapolis, MN, USA), anti-FOXO1 (1:1000; 2880; Cell Signal-

Table 1. Summary of primer sequences used in this study.

Genes		Sequences (5′-3′)
Gapdh	F	GGC ATT GCT CTC AAT GAC AA
	R	CTT GCT CAG TGT CCT TGC TG
Gfap	F	CGA GTC CCT AGA GCG GCA AAT G
	R	GTA GGT GGC GAT CTC GAT GTC
Lcn2	F	CTG AAT GGG TGG TGA GTG TG
	R	GCT CTC TGG CAA CAG GAA AG
Osmr	F	GTG AAG GAC CCA AAG CAT GT
	R	GCC TAA TAC CTG GTG CGT GT
H2D1	F	TCC GAG ATT GTA AAG CGT GAA GA
	R	ACA GGG CAG TGC AGG GAT AG
Serping1	F	ACA GCC CCC TCT GAA TTC TT
	R	GGA TGC TCT CCA AGT TGC TC
Fbln5	F	CTT CAG ATG CAA GCA ACA A
	R	AGG CAG TGT CAG AGG CCT TA
S100a10	F	CCT CTG GCT GTG GAC AAA AT
	R	CTG CTC ACA AGA AGC AGT GG
Clcf1	F	CTT CAA TCC TCC TCG ACT GG
	R	TAC GTC GGA GTT CAG CTG TG
Emp1	F	GAG ACA CTG GCC AGA AAA GC
	R	TAA AAG GCA AGG GAA TGC AC

Gapdh, glyceraldehyde-3-phosphate dehydrogenase; *Gfap*, glial fibrillary acidic protein; *Lcn2,* lipocalin-2; *Osmr*, oncostatin M receptor; *H2D1*, histocompatibility 2, D region locus 1; *Serping1*, serpin family G member 1; *Fbln5*, fibulin 5; *S100a10*, S100 calcium binding protein A10; *Clcf1*, cardiotrophin-like cytokine factor 1; *Emp1*, epithelial membrane protein 1; F, Forward; R, Reverse.

ing Technology, Danvers, MA, USA), anti-phosphorylated cAMP response element-binding protein (pCREB [S133]; 1:2000; 9198; Cell Signaling Technology, Danvers, MA, USA), anti-cAMP response element-binding protein (CREB; 1:2000; 9197; Cell Signaling Technology, Danvers, MA, USA), and anti-β-actin (1:1000; SC-47778; Santa Cruz Biotechnology, Dallas, TX, USA) antibodies. After washing with TBST, the membranes were incubated with horseradish peroxidase-conjugated mouse or rabbit-IgG (1:10,000; ADI-SAB-100-J, ADI-SAB-300-J; Enzo Life Sciences, Farmingdale, NY, USA) in 3% BSA/TBST for 2 h at RT. After washing, the membranes were treated with an enhanced chemiluminescence substrate (2332638; ATTO, Tokyo, Japan) and were visualized using ChemiDoc (version 6.0.1, Bio-Rad, Hercules, CA, USA). Images were quantified using ImageJ (version 1.8.0, National Institutes of Health, Bethesda, MD, USA), if necessary.

Astrocyte Culture

Astroglial-enriched cells were isolated from cortical regions of the mouse brain on postnatal day 1 (P1). These cells were positive for the astrocyte marker, glial fibrillary acidic protein (GFAP), with astrocyte morphology, and were negative for the neuronal marker, βIII-tubulin (TUBB3) [29]. Brains were dissected in sterile Petri dishes containing Hank's Balanced Salt Solution (Gibco™ HBSS; 14175095; Thermo Fisher Scientific, Waltham, MA, USA). The cerebellum, olfactory bulb, and meninges were carefully removed to isolate the cortical regions. Cortices were minced into 1–2 mm fragments and digested using 0.05% trypsin/EDTA (25-053-CI; Corning, Glendale, AZ, USA) at 37 °C for 30 min. Trypsin activity was halted by adding an equal volume of Dulbecco's modified Eagle's medium (Gibco™ DMEM; TFS-12800017; Thermo Fisher Scientific, Waltham, MA, USA) supplemented with 10% fetal bovine serum (Gibco™ FBS; 26140079; Thermo Fisher Scientific, Waltham, MA, USA), 20 mM L-glutamine (25–005-CI; Corning, Glendale, AZ, USA), and 1% antibiotics/antimycotics (30–004-CI; Corning, Glendale, AZ, USA). After centrifugation at 300 $\times$g for 5 min, the supernatant was discarded and the pellet was gently triturated in 5 mL of fresh medium. The suspension was adjusted to 10 mL and transferred to 100 mm poly-D-lysine-coated culture dishes (MW 30,000–70,000; Sigma-Aldrich, St. Louis, MO, USA). The medium was replaced every two days. Confluent astroglial-enriched cells were passaged for 7–8 days and plated onto culture dishes 48 h prior to the experiment. Using a *Mycoplasma* Detection Kit (PP-401L; Jena Bioscience, Thuringia, Germany) and polymerase chain reaction, the cells were confirmed to not be contaminated with *Mycoplasma* based on the absence of an amplified ~270-bp band (16S rRNA coding region of *Mycoplasma*).

Pure Astrocyte Isolation Using Magnetic-Activated Cell Sorting (MACS)

To obtain pure astrocytes, astroglial-enriched cells were purified using MACS by positive selection of astrocytes, while removing microglia, neurons, and other non-neuronal cells. Briefly, the entire hypothalamus was isolated from one-month-old mice and dissociated using an Adult Brain Dissociation Kit (130-107-677; Miltenyi Biotec, Bergisch Gladbach, Germany), according to the manufacturer's protocol. The dissociated lysates were incubated with anti-astrocyte cell surface antigen-2 microbeads (130-092-678; Miltenyi Biotec, Bergisch Gladbach, Germany) for 15 min. Magnetic separation was performed using an LS column (130-042-401; Miltenyi Biotec, Bergisch Gladbach, Germany), according to the manufacturer's instructions. In pure astrocytes, the expression levels of the astrocyte marker *Gfap* were much higher than those of the microglial marker *Tmem119*, as determined by qRT-PCR analysis (Ct [cycle threshold] values for *Gfap* and *Tmem119* were ~23 and ~29, respectively). In addition, even after LPS treatment, LCN2 was not detected in pure astrocytes by western blot analysis because of the absence of microglia. Total RNA was extracted immediately after cell isolation for subsequent analyses.

Statistical Analysis

For multiple comparisons and analyses with more than two groups, a parametric one-way analysis of variance (ANOVA) was performed on data that passed the Shapiro-Wilk normality test and equal variance test, followed by Fisher's least significant difference (LSD) post hoc test. For data that did not follow a normal distribution, a non-parametric one-way ANOVA on ranks (Kruskal-Wallis test) was conducted, followed by the Student-Newman-Keuls post hoc test. For the comparison between two groups, two-tailed unpaired Student's *t* test was performed on data that passed the Shapiro-Wilk normality test. All statistical analyses were performed using SigmaPlot 14.5 software (Systat Software Inc, San Jose, CA, USA). Differences between the two groups were considered statistically significant at $p < 0.05$.

Results

Reactive Astrogliosis and Neuroinflammatory Phenotypes in Young Ubb KO Mice

RNA-seq analysis was performed using RNA isolated from the hypothalamus of young (one-month-old) and adult (three-month-old) WT and *Ubb* KO mice (Fig. 1A). Most astrocyte activation markers were dramatically elevated in young (one-month-old) *Ubb* KO mice compared with those in WT mice (Fig. 1B, 1 M *Ubb* KO vs 1 M WT). These markers included pan, neurotoxic A1, and neuroprotective A2 markers. However, by three months of age, the expression levels decreased and were only slightly higher than or comparable with those in the WT mice (Fig. 1B, 3 M *Ubb* KO vs 3 M WT).

Although LCN2 is classified as a pan-marker, it exhibits neurotoxic effects when secreted by activated astrocytes [30]. *Lcn2* expression is typically high in activated astrocytes expressing high levels of the A1 marker. In this study, *Lcn2* expression levels were much higher in young (one-month-old) *Ubb* KO mice than in age-matched WT mice (Fig. 1B, 1 M *Ubb* KO vs 1 M WT, arrowhead). However, at three months of age, *Lcn2* expression levels were not significantly different between WT and *Ubb* KO mice (Fig. 1B, 3 M *Ubb* KO vs 3 M WT, arrowhead). In addition, when astrocytes from the hypothalamus of young (one-month-old) mice were purified using MACS, they exhibited a similar trend, with increased astrocyte activation marker expression in *Ubb* KO mice (Fig. 1C). This indicates that the elevated *Lcn2* expression in young *Ubb* KO mice is a cell-autonomous effect and not merely a reflection of an increased number of glial cells. The RNA-seq data was further validated using qRT-PCR (Fig. 2A–C). Although there was variability among individual mice, the overall trend showed more prominent astrocyte activation in young (one-month-old) *Ubb* KO mice.

Intrinsic Inflammatory Stress in Young Ubb KO Mice Without Exposure to Inflammatory Stressors

Next, the ability of peripheral intraperitoneal LPS administration to further enhance *Lcn2* and other neuroinflammatory markers in young (one-month-old) *Ubb* KO mice was investigated. Systemic LPS injection dramatically increases *Lcn2* and pan and A1 marker expression levels in the brain [31]. In young (one-month-old) *Ubb* KO mice, similar trends in *Lcn2* expression levels were observed following LPS administration, although statistical significance could not be achieved owing to variability among individual mice (Fig. 3A, $p = 0.09$). Pan and A1 marker expression levels also showed similar upward trends in young *Ubb* KO mice after LPS challenge (Fig. 3A,B). However, similar trends in neuroinflammatory markers were observed in age-matched WT mice after the LPS challenge (Fig. 3A,B). Thus, there was no discernible difference between the WT and *Ubb* KO mice in response to LPS. LPS-induced upregulation of pan and A1 marker expression was statistically significant in 4 out of 6 markers in WT mice and 2 out of 6 markers in *Ubb* KO mice (Fig. 3A,B). Although other markers also showed similar upward trends, statistical significance could not be achieved owing to variability among individual mice. As expected, the A2 marker expression remained almost unresponsive to LPS in both WT and *Ubb* KO mice (Fig. 3C).

Even without LPS exposure, *Lcn2* and other neuroinflammatory markers were elevated in young (one-month-old) *Ubb* KO mice, suggesting that young *Ubb* KO mice were under intrinsic inflammatory stress. We then used cultured astrocytes isolated from the mouse brain on P1. After verifying that these cells were positive for GFAP and negative for TUBB3 by immunofluorescence analysis, the cultured cells were considered astrocytes [29]. LCN2 protein levels in cultured astrocytes isolated from WT and *Ubb* KO mice at P1 were compared. As expected, the LCN2 protein levels were undetectable by western blot analysis in the absence of LPS (Fig. 4A). Following LPS treatment, LCN2 protein was detected in both WT and *Ubb* KO astrocytes, but the levels were not significantly different (Fig. 4A,B, $p = 0.14$). *Lcn2* expression in cultured *Ubb* KO astrocytes was comparable with that in WT astrocytes without LPS treatment (Fig. 4C). Upon LPS exposure, both WT and *Ubb* KO astrocytes exhibited a dramatic increase in *Lcn2* expression levels of more than 1000-fold (Fig. 4C, $p < 0.001$). In contrast to cultured astrocytes isolated on P1, basal *Lcn2* expression levels in purified astrocytes and in the hypothalamus were higher in young (one-month-old) *Ubb* KO mice than in WT mice (see Fig. 1). This suggests that basal *Lcn2* expression continues to increase during early development in *Ubb* KO mice, which may be sufficient to induce chronic neuroinflammation, even without external stressors. These results indicated that young *Ubb* KO mice were under intrinsic inflammatory stress with astrocyte activation and increased LCN2 secretion. Hence, elevated LCN2 levels may

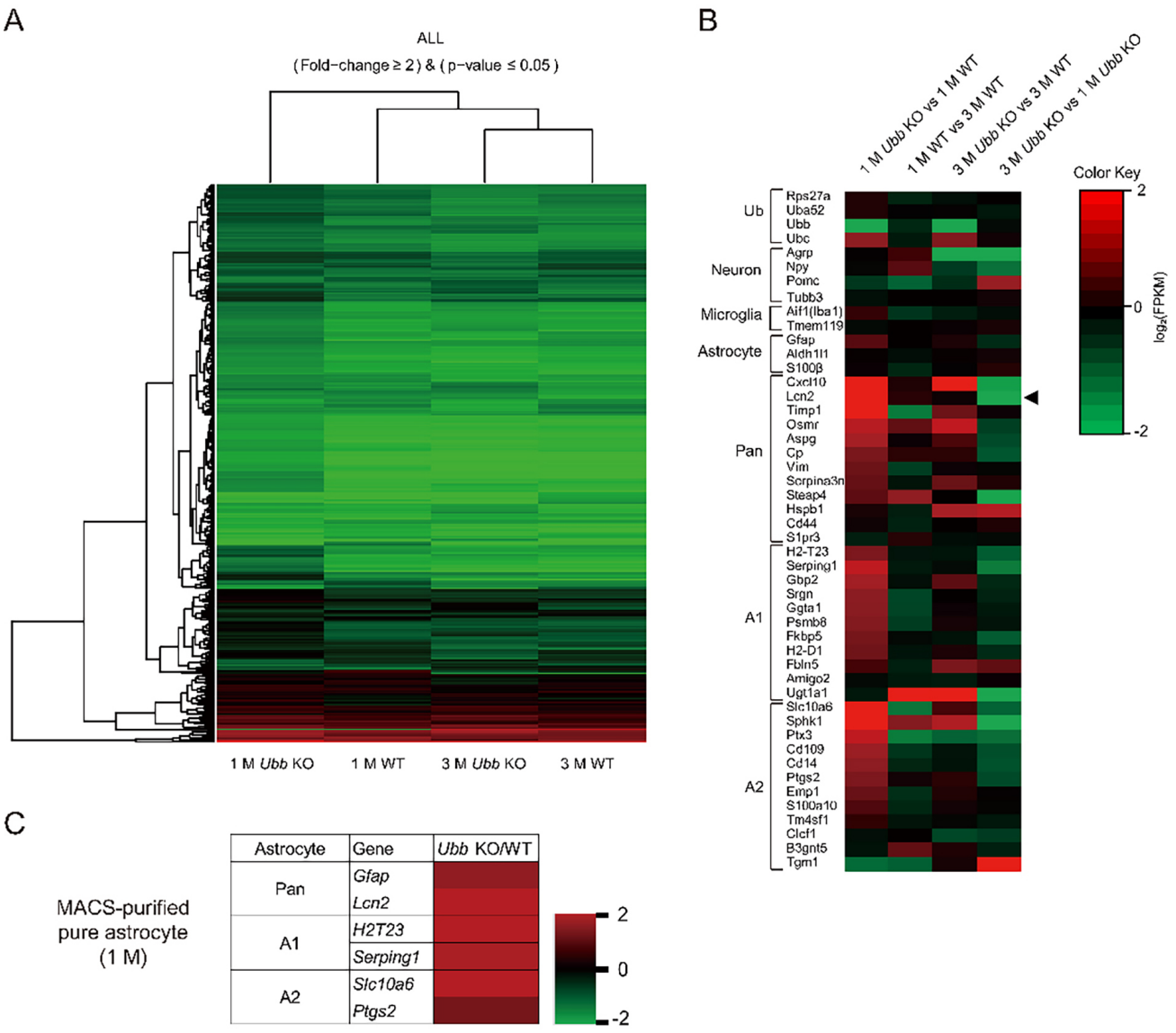

Fig. 1. Upregulation of reactive astrogliosis markers in young *Ubb* knockout (KO) mice. (A) Hierarchical clustering of gene expression profiles. (B) Heatmap representation of RNA-seq data showing differentially expressed gene (DEG) in the hypothalamus of young (1 M, one-month-old) vs. adult (3 M, three-month-old) wild-type (WT) and *Ubb* KO mice. (C) Heatmap representation of quantitative reverse transcription-polymerase chain reaction (qRT-PCR) results from magnetic-activated cell sorting (MACS)-purified pure astrocytes. Astrocytes were obtained from young (one-month-old) WT and *Ubb* KO mice.

act as an anorexigenic signal, thereby reducing food intake and resulting in impaired body weight gain.

Leptin Signaling Dysfunction in Adult Ubb KO Mice Due to Increased SOCS3 and FOXO1 Levels

When mice were treated with leptin for 1 h via an IP injection after fasting for 24 h, STAT3 phosphorylation was observed in the arcuate nucleus (ARC) of the hypothalamus of both WT and *Ubb* KO mice at one month of age (Fig. 5A). These results suggested that leptin signaling was intact in young *Ubb* KO mice. Therefore, intrinsic inflammatory stress in young *Ubb* KO mice does not impair leptin signaling. However, when the mice reached adulthood, pSTAT3-positive cells could not be easily identified in the ARC of the hypothalamus after leptin administration in *Ubb* KO mice, in contrast to WT mice (Fig. 5B). As STAT3 phosphorylation is a key factor in the inflammatory signaling pathway, using it solely as a marker to assess the integrity of leptin signaling may warrant further clarification. Serum leptin levels are elevated because the leptin receptor is unresponsive, thereby contributing to obesity and increased fat content. Furthermore, LCN2 levels were reduced in adult *Ubb* KO mice compared with those in young *Ubb* KO mice, thus weakening the anorexigenic effect of LCN2 and promoting obesity in *Ubb* KO mice.

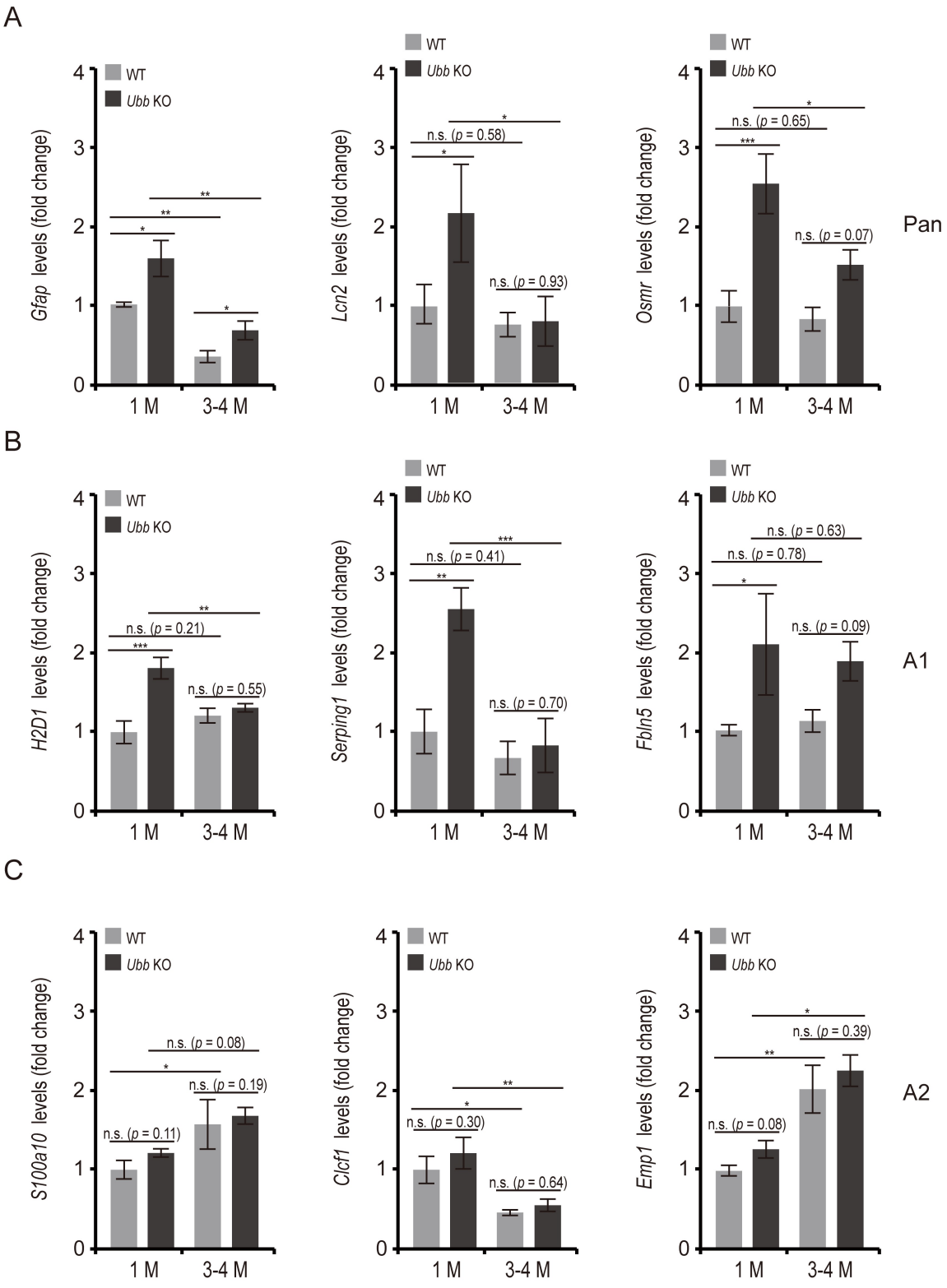

Fig. 2. Confirmation of the upregulation of reactive astrogliosis markers in young *Ubb* KO mice. (A) Expression levels of pan-astrocyte markers (*Gfap*, *Lcn2*, *Osmr*) were determined using qRT-PCR, normalized to *Gapdh* levels, and expressed as fold change relative to the control (1 M, one-month-old WT mice; n = 4). (B) Expression levels of A1 astrocyte markers (*H2D1*, *Serping1*, *Fbln5*) were determined as described above (n = 4). (C) Expression levels of A2 astrocyte markers (*S100a10*, *Clcf1*, *Emp1*) were also determined similarly (n = 4). Data are expressed as means ± standard error of the mean (SEM) from four independent sets of mice using one-way analysis of variance (ANOVA), followed by post hoc multiple comparison test. *$p < 0.05$, **$p < 0.01$, ***$p < 0.001$ between two groups as indicated by the horizontal bars. n.s., not significant.

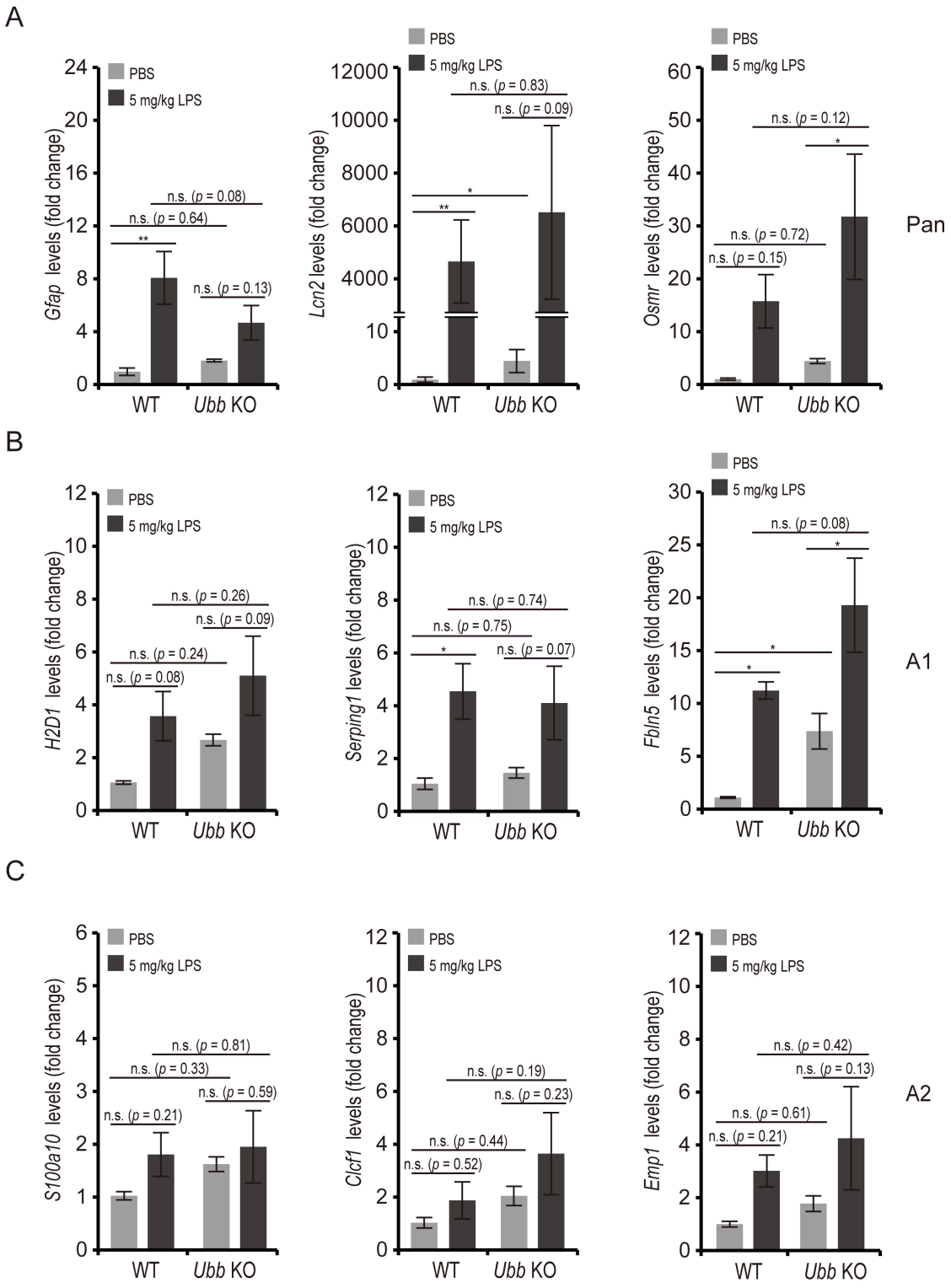

Fig. 3. Upregulation of reactive astrogliosis markers in WT and *Ubb* knockout (KO) mice upon lipopolysaccharide (LPS) challenge. (A) Young (one-month-old) WT and *Ubb* KO mice were treated with LPS (5 mg/kg body weight) via intraperitoneal (IP) injection. One day later, RNA was isolated from the brain, and expression levels of pan-astrocyte markers (*Gfap*, *Lcn2*, *Osmr*) were determined using qRT-PCR, normalized to *Gapdh* levels, and expressed as fold change relative to the control (WT mice, phosphate-buffered saline [PBS]-treated; n = 3). (B) Expression levels of A1 astrocyte markers (*H2D1*, *Serping1*, *Fbln5*) were determined as described above (n = 3). (C) Expression levels of A2 astrocyte markers (*S100a10*, *Clcf1*, *Emp1*) were also determined similarly (n = 3). Data are expressed as means ± standard error of the mean (SEM) from three independent sets of mice using one-way ANOVA, followed by post hoc multiple comparison test. *$p < 0.05$, **$p < 0.01$ between two groups as indicated by the horizontal bars. n.s., not significant.

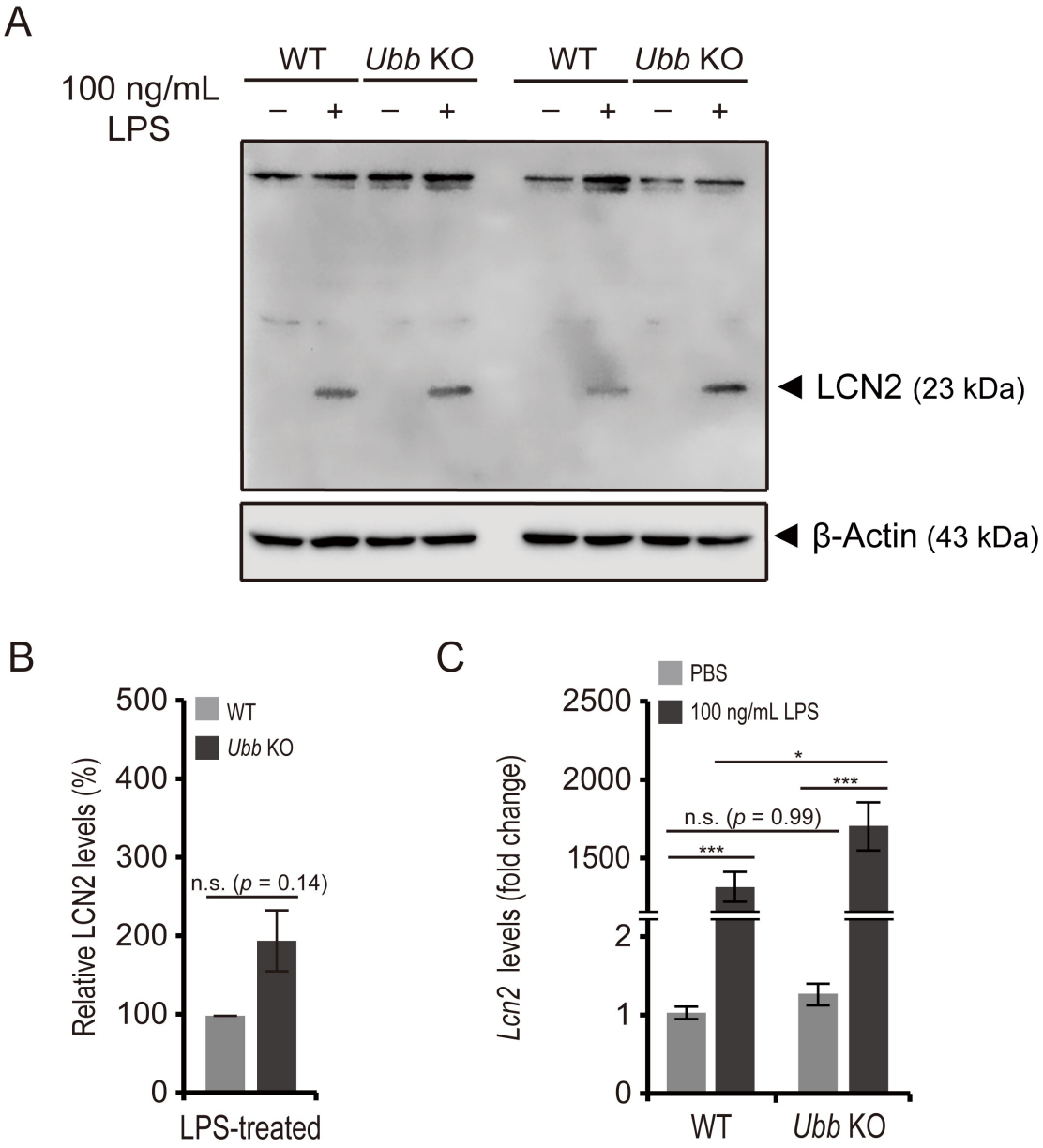

Fig. 4. Detection of LCN2 in WT and *Ubb* KO astrocytes upon lipopolysaccharide (LPS) treatment. (A) Primary astrocyte cultures were prepared from WT and *Ubb* KO mouse brains at postnatal day 1 (P1). Astrocytes were treated with LPS (100 ng/mL) for one day, and western blot analysis was performed to detect LCN2. β-actin was used as a loading control. Western blot results from two independent sets of mice are shown. (B) LCN2 band intensities in the presence of LPS (100 ng/mL) were normalized to β-actin and expressed as fold change relative to the corresponding control (WT astrocytes from P1, LPS-treated, n = 3). Quantification of band intensities was carried out using ImageJ software (version 1.8.0, National Institutes of Health, Bethesda, MD, USA). (C) RNA was isolated from WT and *Ubb* KO astrocytes treated with LPS as described above, and *Lcn2* expression was determined using qRT-PCR, normalized to *Gapdh* levels, and expressed as fold change relative to the control (WT astrocytes from P1, PBS-treated; n = 3). Data in (B) and (C) are expressed as means $\pm$ SEM from three independent sets of mice using two-tailed unpaired *t*-test (B) or one-way ANOVA, followed by post hoc multiple comparison test (C). $*p < 0.05$, $***p < 0.001$ between two groups as indicated by the horizontal bars. n.s., not significant.

To directly assess the effect of leptin, leptin was administered via ICV injection during refeeding after fasting for 24 h. Leptin was administered during the last 2 h of the 6 h refeeding period (Fig. 6A). As expected, leptin administration during refeeding increased the levels of negative regulators of leptin signaling as part of feedback regulation, which was also observed in WT mice. In *Ubb* KO mice, SOCS3 and FOXO1 levels were significantly higher than those in WT mice ($p < 0.01$) and were not largely affected by leptin administration, which likely suppressed the acti-

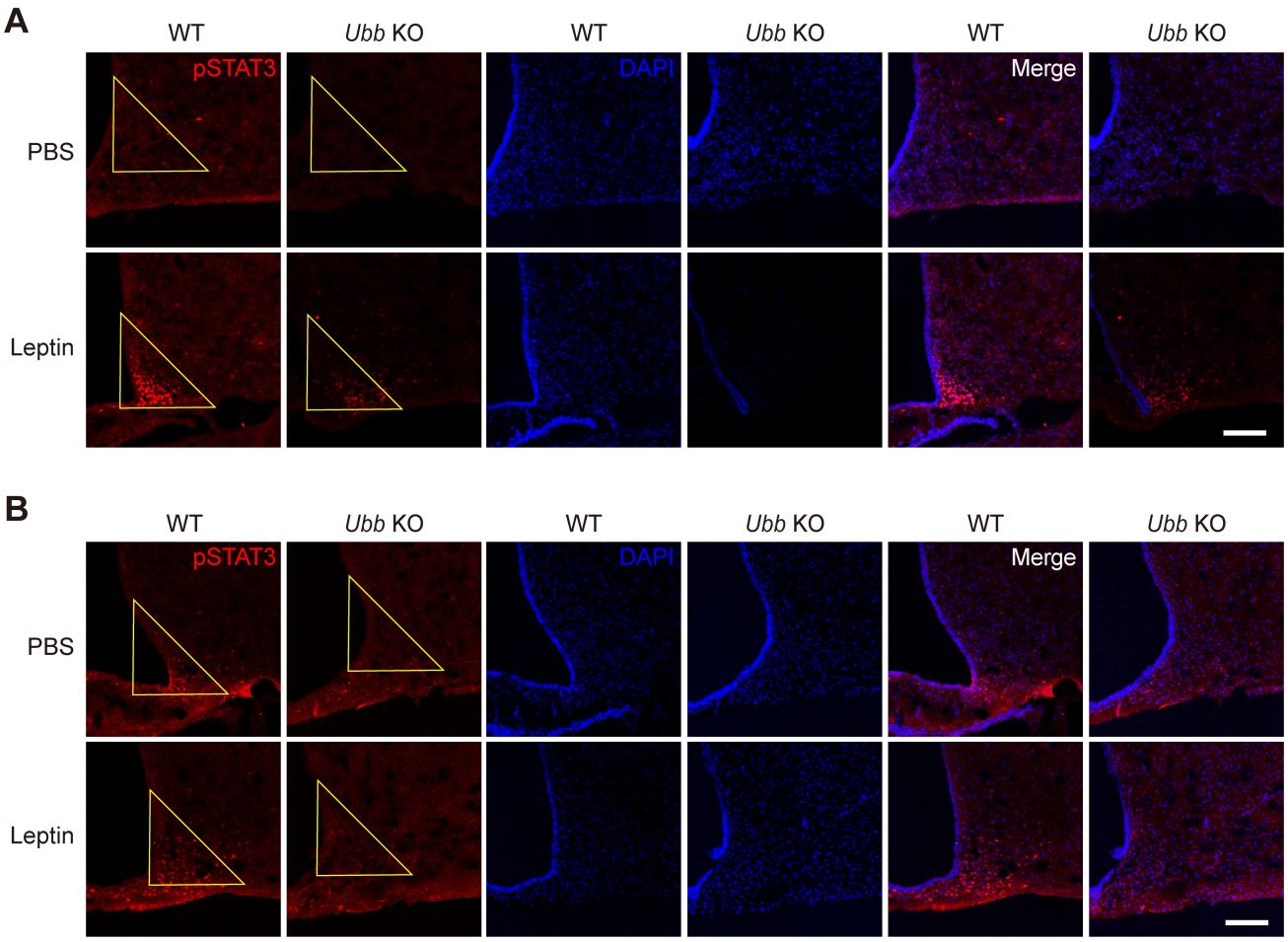

Fig. 5. No signal transducer and activator of transcription-3 (STAT3) phosphorylation in adult *Ubb* KO mice after leptin administration. (A) Young (one-month-old) WT and *Ubb* KO mice were fasted for 24 h and treated with leptin (1 mg/kg body weight) via IP injection. After 1 h, the mice were sacrificed, and coronal brain sections (25 µm thick, 1.9 mm posterior to bregma) were prepared. Following leptin treatment, phosphorylated STAT3 (pSTAT3)-positive cells were observed in the arcuate nucleus (ARC) of the hypothalamus in both WT and *Ubb* KO mice. (B) Adult (three- to four-month-old) WT and *Ubb* KO mice were treated with leptin and the brain sections were prepared as described above. In adult mice treated with leptin, pSTAT3-positive cells were not well observed in the ARC of the hypothalamus in *Ubb* KO mice, in contrast to WT mice. Yellow triangles indicate the ARC area. Representative immunofluorescence results from two independent sets of mice are shown. Scale bar, 100 µm.

vation of leptin signaling (Fig. 6B,C). Consistent with previous reports [32,33], the elevated expression of *Socs3* and *Foxo1* may be driven by high pCREB levels, which function as a transcription factor for these genes (Fig. 6B,C). Therefore, in adult *Ubb* KO mice, both impaired leptin signaling and reduced LCN2 levels contribute to increased body weight and obesity.

Discussion

Early onset reactive astrogliosis, adult-onset hypothalamic neurodegeneration, and obesity in *Ubb* KO mice appear to be distinct events, although reactive astrogliosis can lead to neurodegeneration [9]. LCN2 levels increase when astrocytes are activated; however, after neurodegeneration occurs owing to the neurotoxic function of LCN2, LCN2 levels are subsequently reduced [34–36]. Therefore, it is not surprising that young *Ubb* KO mice exhibit higher LCN2 levels, whereas adult *Ubb* KO mice show lower LCN2 levels. Furthermore, the connection between hypothalamic neurodegeneration and the obesity phenotype is not clear. Thus, this study proposes a link between the distinct phenotypes observed in young and adult *Ubb* KO mice. Although a closer examination of daily food intake and LCN2 levels in individual mice of different ages may be required, the reduced body weight of young *Ubb* KO mice may be primarily attributed to elevated LCN2 levels, as leptin signaling remains intact. Their daily food intake likely increased gradually until they reached a body weight comparable with that of WT mice, as supported by the reduction in LCN2 levels observed in adult *Ubb* KO mice. LCN2 serves as an anorexigenic signal to suppress appetite

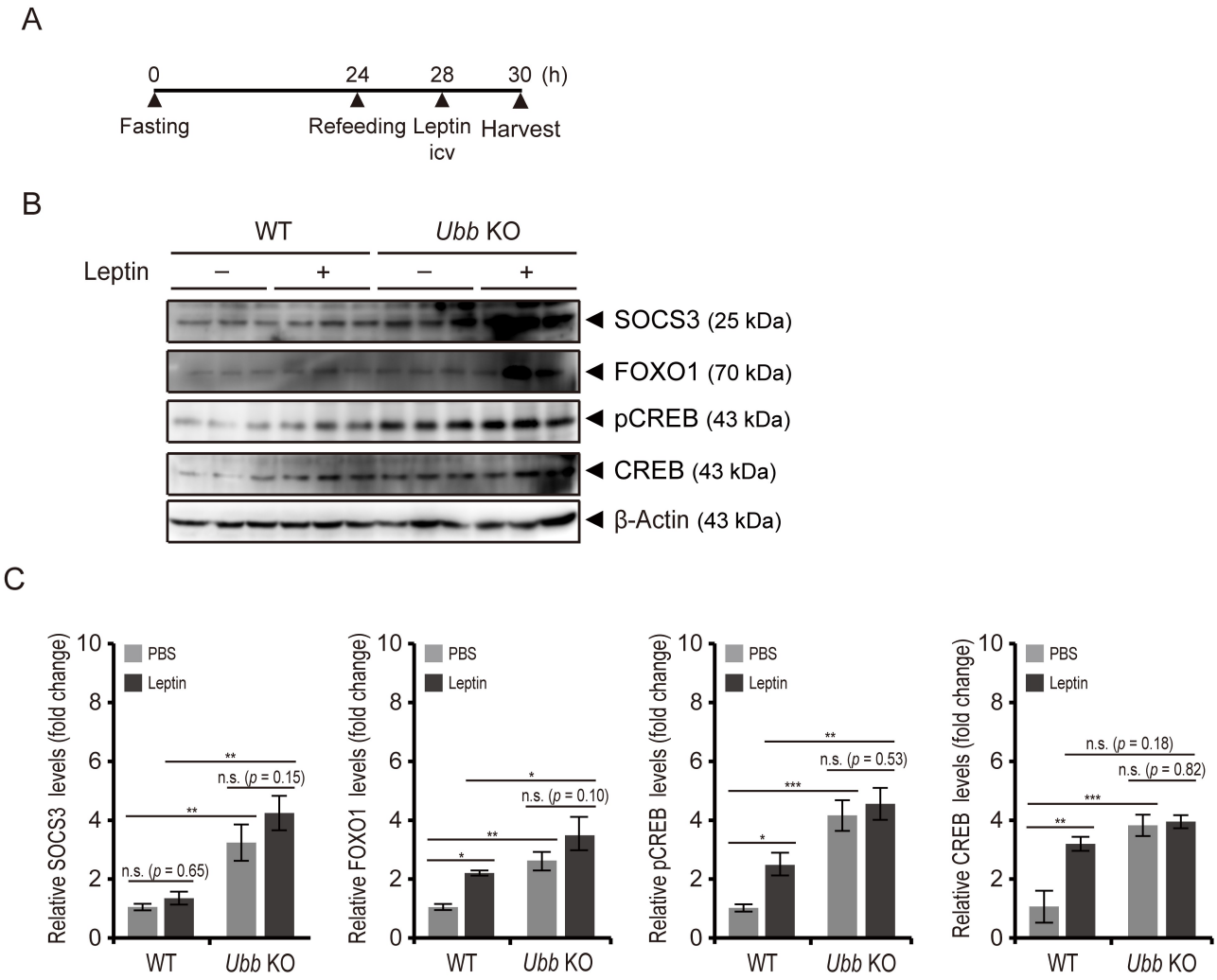

Fig. 6. Increased levels of negative regulators of leptin signaling in adult *Ubb* KO mice. (A) Experimental scheme. Adult (three- to four-month-old) WT and *Ubb* KO mice were fasted for 24 h and refed for 6 h. Leptin (1 µg) was administered via intracerebroventricular (ICV) injection at the indicated time point. After 2 h, the mice were sacrificed, and the hypothalamus was collected. (B) Western blot detection of suppressor of cytokine signaling-3 (SOCS3), forkhead box protein O1 (FOXO1), phosphorylated cAMP response element-binding protein (pCREB), and total CREB (CREB) in WT and *Ubb* KO hypothalamus with or without leptin administration. β-actin was used as a loading control. Western blot results from three independent sets of mice are shown. (C) SOCS3, FOXO1, pCREB, and CREB band intensities were normalized to β-actin and expressed as fold change relative to the control (adult WT mice, PBS-treated, n = 3). Data in (C) are expressed as means ± standard error of the mean (SEM) from three independent sets of mice using one-way ANOVA, followed by post hoc multiple comparison test. $^{*}p < 0.05$, $^{**}p < 0.01$, $^{***}p < 0.001$ between two groups as indicated by the horizontal bars. n.s., not significant.

in mice [19,21]. Similarly, young and adult *Ubb* KO mice exhibited high and low LCN2 levels, respectively.

Adult *Ubb* KO mice previously exhibited reduced compensatory hyperphagic behavior after fasting and refeeding compared with that in WT mice [9]. This suggests that *Ubb* KO mice may have impaired recognition of fasting states, resulting in reduced food consumption, even when food is available during the refeeding period. This behavior is likely owing to dysfunctional leptin signaling and consistently high serum leptin levels, regardless of the fasting or feeding status. Normally, serum leptin levels decrease during fasting; however, this regulation appears to be disrupted in *Ubb* KO mice. In addition, although we suggested that leptin signaling is impaired in adult *Ubb* mice, since STAT3 phosphorylation is a key factor in the inflammatory signaling pathway, using it solely as a marker to assess the integrity of leptin signaling has some limitations and may warrant further clarification.

Considering that reactive astrogliosis is most prominent in the hypothalamus, chronic neuroinflammation is likely to have a particularly profound effect in this brain region. Elevated levels of negative regulators of leptin sig-

naling, such as SOCS3 and FOXO1, may contribute to the impaired leptin signaling observed in adult *Ubb* KO mice. Although this is beyond the scope of the current study, more direct evidence is needed to determine the reason SOCS3 and FOXO1 levels are elevated in adult *Ubb* KO mice, and whether their expression is indeed upregulated by pCREB. In addition, the signaling pathways that lead to CREB phosphorylation need to be investigated. Examining whether the increased levels of these negative regulators are related to the reduced availability of free Ub will also be worthwhile. Reduced availability of free Ub may impair the degradation of target proteins by the proteasome because both SOCS3 and FOXO1 are known to be degraded by the proteasome [37,38]. Elevated levels of these negative regulators and their relationship with chronic neuroinflammation, along with the underlying molecular mechanisms, should be explored in future studies.

Furthermore, hypothalamic neurodegeneration in adult *Ubb* KO mice may reduce the population of neurons that express leptin receptors. Although leptin receptor expression levels in the hypothalamus were similar between WT and *Ubb* KO mice (unpublished observation), the total number of neurons was reduced in adult *Ubb* KO mice. This reduction may result in increased leptin receptor expression in the remaining neurons. Nevertheless, high levels of negative regulators, such as SOCS3 and FOXO1, most likely render leptin signaling unresponsive in *Ubb* KO mice.

Conclusion

This study demonstrated that early onset astrocyte activation increases *Lcn2* expression. Although leptin signaling remains intact in young *Ubb* KO mice, elevated LCN2 levels may contribute to decreased daily food intake, leading to reduced body weight. Chronic neuroinflammation resulting from reactive astrogliosis impairs leptin signaling by increasing the levels of SOCS3 and FOXO1, both of which are negative regulators of leptin signaling. Consequently, leptin receptors become unresponsive, resulting in elevated serum leptin levels in adult *Ubb* KO mice.

Availability of Data and Materials

The datasets used and/or analyzed during the current study are available from the corresponding author upon reasonable request.

Author Contributions

JSB, SY, and KYR designed the study. JSB and SY performed the mouse experiments, qRT-PCR, western blot, and immunofluorescence analyses. TYK analyzed the immunofluorescence data. KYR supervised the experiments, interpreted the data, and wrote the manuscript. All authors contributed significantly to editorial changes of important content. All authors have participated sufficiently in the work and agreed to be accountable for all aspects of the work. All the authors have read and approved the final manuscript.

Ethics Approval and Consent to Participate

All the animal experiments were approved by the University of Seoul Institutional Animal Care and Use Committee (approval no. UOS-IACUC-2020-03-A, UOS IACUC-2021-01-TA, UOS-IACUC-2023-05).

Acknowledgment

Not applicable.

Funding

This work was supported by the National Research Foundation of Korea (NRF) grant funded by the Korea government (MSIT) (No. 2023R1A2C1004447) to KYR.

Conflict of Interest

The authors declare no conflict of interest.

References

[1] Damgaard RB. The ubiquitin system: from cell signalling to disease biology and new therapeutic opportunities. Cell Death and Differentiation. 2021; 28: 423–426.

[2] Li Y, Li S, Wu H. Ubiquitination-Proteasome System (UPS) and Autophagy Two Main Protein Degradation Machineries in Response to Cell Stress. Cells. 2022; 11: 851.

[3] Liao Y, Zhang W, Liu Y, Zhu C, Zou Z. The role of ubiquitination in health and disease. MedComm. 2024; 5: e736.

[4] Kim AH, Chiknas PM, Lee REC. Ubiquitin: Not just a one-way ticket to the proteasome, but a therapeutic dial to fine-tune the molecular landscape of disease. Clinical and Translational Medicine. 2024; 14: e1769.

[5] Dewson G, Eichhorn PJA, Komander D. Deubiquitinases in cancer. Nature Reviews. Cancer. 2023; 23: 842–862.

[6] Eastham MJ, Pelava A, Wells GR, Watkins NJ, Schneider C. RPS27a and RPL40, Which Are Produced as Ubiquitin Fusion Proteins, Are Not Essential for p53 Signalling. Biomolecules. 2023; 13: 898.

[7] Gemayel R, Yang Y, Dzialo MC, Kominek J, Vowinckel J, Saels V, *et al*. Variable repeats in the eukaryotic polyubiquitin gene ubi4 modulate proteostasis and stress survival. Nature Communications. 2017; 8: 397.

[8] Kobayashi M, Oshima S, Maeyashiki C, Nibe Y, Otsubo K, Matsuzawa Y, *et al*. The ubiquitin hybrid gene UBA52 regulates ubiquitination of ribosome and sustains embryonic development. Scientific Reports. 2016; 6: 36780.

[9] Ryu KY, Garza JC, Lu XY, Barsh GS, Kopito RR. Hypothalamic neurodegeneration and adult-onset obesity in mice lacking the Ubb polyubiquitin gene. Proceedings of the National Academy of Sciences of the United States of America. 2008; 105: 4016–4021.

[10] Ryu KY, Fujiki N, Kazantzis M, Garza JC, Bouley DM, Stahl A, *et al*. Loss of polyubiquitin gene Ubb leads to metabolic and sleep abnormalities in mice. Neuropathology and Applied Neurobiology. 2010; 36: 285–299.

[11] Gruzdeva O, Borodkina D, Uchasova E, Dyleva Y, Barbarash O. Leptin resistance: underlying mechanisms and diagnosis. Diabetes, Metabolic Syndrome and Obesity: Targets and Therapy. 2019; 12: 191–198.

[12] Obradovic M, Sudar-Milovanovic E, Soskic S, Essack M, Arya S, Stewart AJ, *et al*. Leptin and Obesity: Role and Clinical Implication. Frontiers in Endocrinology. 2021; 12: 585887.

[13] Liu H, Du T, Li C, Yang G. STAT3 phosphorylation in central leptin resistance. Nutrition & Metabolism. 2021; 18: 39.

[14] Liddelow SA, Guttenplan KA, Clarke LE, Bennett FC, Bohlen CJ, Schirmer L, *et al*. Neurotoxic reactive astrocytes are induced by activated microglia. Nature. 2017; 541: 481–487.

[15] Li K, Li J, Zheng J, Qin S. Reactive Astrocytes in Neurodegenerative Diseases. Aging and Disease. 2019; 10: 664–675.

[16] Liddelow SA, Barres BA. Reactive Astrocytes: Production, Function, and Therapeutic Potential. Immunity. 2017; 46: 957–967.

[17] Escartin C, Galea E, Lakatos A, O'Callaghan JP, Petzold GC, Serrano-Pozo A, *et al*. Reactive astrocyte nomenclature, definitions, and future directions. Nature Neuroscience. 2021; 24: 312–325.

[18] Sofroniew MV. Astrocyte Reactivity: Subtypes, States, and Functions in CNS Innate Immunity. Trends in Immunology. 2020; 41: 758–770.

[19] Olson B, Zhu X, Norgard MA, Levasseur PR, Butler JT, Buenafe A, *et al*. Lipocalin 2 mediates appetite suppression during pancreatic cancer cachexia. Nature Communications. 2021; 12: 2057.

[20] Petropoulou PI, Mosialou I, Shikhel S, Hao L, Panitsas K, Bisikirska B, *et al*. Lipocalin-2 is an anorexigenic signal in primates. eLife. 2020; 9: e58949.

[21] Yang Y, Liu J, Kousteni S. Lipocalin 2-A bone-derived anorexigenic and β-cell promoting signal: From mice to humans. Journal of Diabetes. 2024; 16: e13504.

[22] Carow B, Rottenberg ME. SOCS3, a Major Regulator of Infection and Inflammation. Frontiers in Immunology. 2014; 5: 58.

[23] Chaves de Souza JA, Nogueira AVB, Chaves de Souza PP, Kim YJ, Silva Lobo C, Pimentel Lopes de Oliveira GJ, *et al*. SOCS3 expression correlates with severity of inflammation, expression of proinflammatory cytokines, and activation of STAT3 and p38 MAPK in LPS-induced inflammation in vivo. Mediators of Inflammation. 2013; 2013: 650812.

[24] Liu J, Lai F, Hou Y, Zheng R. Leptin signaling and leptin resistance. Medical Review (2021). 2022; 2: 363–384.

[25] Liu Z, Xiao T, Liu H. Leptin signaling and its central role in energy homeostasis. Frontiers in Neuroscience. 2023; 17: 1238528.

[26] Sawoo R, Bishayi B. TLR4/TNFR1 blockade suppresses STAT1/STAT3 expression and increases SOCS3 expression in modulation of LPS-induced macrophage responses. Immunobiology. 2024; 229: 152840.

[27] Wang Z, do Carmo JM, da Silva AA, Bailey KC, Aberdein N, Moak SP, *et al*. Role of SOCS3 in POMC neurons in metabolic and cardiovascular regulation. American Journal of Physiology. Regulatory, Integrative and Comparative Physiology. 2019; 316: R338–R351.

[28] Liu X, Zheng H. Modulation of Sirt1 and FoxO1 on Hypothalamic Leptin-Mediated Sympathetic Activation and Inflammation in Diet-Induced Obese Rats. Journal of the American Heart Association. 2021; 10: e020667.

[29] Jung BK, Park Y, Yoon B, Bae JS, Han SW, Heo JE, *et al*. Reduced secretion of LCN2 (lipocalin 2) from reactive astrocytes through autophagic and proteasomal regulation alleviates inflammatory stress and neuronal damage. Autophagy. 2023; 19: 2296–2317.

[30] Murray TE, Richards CM, Robert-Gostlin VN, Bernath AK, Lindhout IA, Klegeris A. Potential neurotoxic activity of diverse molecules released by astrocytes. Brain Research Bulletin. 2022; 189: 80–101.

[31] Bae JS, Heo JE, Ryu KY. Proteasome inhibition suppresses the induction of lipocalin-2 upon systemic lipopolysaccharide challenge in mice. Molecular Brain. 2024; 17: 73.

[32] Wondisford AR, Xiong L, Chang E, Meng S, Meyers DJ, Li M, *et al*. Control of Foxo1 gene expression by co-activator P300. The Journal of Biological Chemistry. 2014; 289: 4326–4333.

[33] Yang L, McKnight GS. Hypothalamic PKA regulates leptin sensitivity and adiposity. Nature Communications. 2015; 6: 8237.

[34] Choi J, Lee HW, Suk K. Increased plasma levels of lipocalin 2 in mild cognitive impairment. Journal of the Neurological Sciences. 2011; 305: 28–33.

[35] das Neves SP, Taipa R, Marques F, Soares Costa P, Monárrez-Espino J, Palha JA, *et al*. Association Between Iron-Related Protein Lipocalin 2 and Cognitive Impairment in Cerebrospinal Fluid and Serum. Frontiers in Aging Neuroscience. 2021; 13: 663837.

[36] Li X, Wang X, Guo L, Wu K, Wang L, Rao L, *et al*. Association between lipocalin-2 and mild cognitive impairment or dementia: A systematic review and meta-analysis of population-based evidence. Ageing Research Reviews. 2023; 89: 101984.

[37] Jiang Z, Xing B, Feng Z, Ma J, Ma X, Hua X. Menin Upregulates FOXO1 Protein Stability by Repressing Skp2-Mediated Degradation in β Cells. Pancreas. 2019; 48: 267–274.

[38] Klepsch O, Namer LS, Köhler N, Kaempfer R, Dittrich A, Schaper F. Intragenic regulation of SOCS3 isoforms. Cell Communication and Signaling: CCS. 2019; 17: 70.